

Supplementary Information

Cyano-disubstituted dipyrrolopyrazinedione (CNPzDP) small molecules for solution processed n-channel organic thin-film transistors

Wei Hong,^a Chang Guo,^a Bin Sun,^a Zhuangqing Yan,^a Chun Huang,^b Yan Hu,^b Yan Zheng,^b
Antonio Facchetti,^b Yuning Li^{*a}

^a Department of Chemical Engineering and Waterloo Institute for nanotechnology (WIN), University of Waterloo, 200 University Ave West, Waterloo, ON, Canada, N2L 3G1. E-mail: yuning.li@uwaterloo.ca.

^b Polyera Corporation, 8045 Lamon Avenue, Skokie, IL 60077, USA.

Contents

1. Materials and Characterization

2. Synthetic Procedures

3. Additional data: Computer simulation results, ¹H-NMR and ¹³C-NMR spectra, thermal gravimetric analysis (TGA), differential scanning calorimetry (DSC), and ultraviolet and visible absorption (UV-Vis) spectra.

4. References

Supplementary Information

1. Materials and Characterization

Reagents and solvents were purchased from commercial resources and used as received. 3,7-Bis(4-bromophenyl)dipyrrolo[2,3-*b*:2',3'-*e*]pyrazine-2,6(1*H*,5*H*)-dione (compound **1**)¹ were synthesized according to the literature method. NMR data were recorded on a Bruker DPX 300 MHz spectrometer. The chemical shifts were reported relative to an internal reference, tetramethylsilane (TMS, 0 ppm). UV-Vis spectra were recorded on a Thermo Scientific Genesys 10 UV instrument. Differential scanning calorimetry (DSC) measurements were carried out on a TA Instruments DSC Q2000 at a scanning rate of 10 °C·min⁻¹ under nitrogen. Thermal gravimetric analysis (TGA) was carried out using a TA Instruments SDT 2960 at a heating rate of 10 °C·min⁻¹ under nitrogen. Cyclic voltammetry (CV) measurements were performed on a BAS-CV-50W potentiostat/galvanostat using an Ag/AgCl reference electrode, a Pt wire counter electrode, and a Pt foil working electrode. CV measurements were recorded in 0.1 M tetrabutylammonium hexafluorophosphate in anhydrous dichloromethane at a sweeping rate of 50 mV·s⁻¹ under nitrogen, using the ferrocene/ferrocenium (Fc/Fc⁺) couple (with a ionization potential of 4.8 eV)^{1,2} as an internal reference. The LUMO energy levels were estimated using the equations of $E_{\text{LUMO}} \text{ (eV)} = E_{\text{redox}}^{0/-} - 4.8 \text{ eV} = 1/2(E_{\text{pa}}^{0/-} + E_{\text{pc}}^{0/-}) - 4.8 \text{ eV}$, where $E_{\text{redox}}^{0/-}$ was the half-wave potential values, and $E_{\text{pa}}^{0/-}$ and $E_{\text{pc}}^{0/-}$ are the first peak oxidation and reduction potentials, respectively. X-ray diffraction (XRD) diagrams of **3b** thin film were obtained with a Bruker D8 Advance powder diffractometer using standard Bragg-Brentano geometry with Cu K α radiation ($\lambda = 1.5406 \text{ \AA}$). The **3b** thin film (~100 nm) for the XRD analysis were deposited by spin-coating **3b** solution in 1,2-dichlorobenzene (DCB) on glass wafer (Precision Glass & Optics, Eagle 2000) coated with polyolefin-polyacrylate buffer (Polyera ActiveInkTM B2000). Atomic force microscopic (AFM) images were obtained from **3a** and **3b** thin films on glass substrates using a Dimension 3100 Scanning Probe Microscope. The thin films (~30-40 nm) on glass substrates for the AFM analysis were deposited by spin-coating the semiconductor solutions in DCB.

Supplementary Information

Computer calculations of 3,7-bis(phenyl)-1,5-dimethyldipyrrolo[2,3-b:2',3'-e]pyrazine-2,6(1*H*,5*H*)-dione (PzDP-Me) and 3,7-bis(4-cyanophenyl)-1,5-dimethyldipyrrolo[2,3-b:2',3'-e]pyrazine-2,6(1*H*,5*H*)-dione (CNPzDP-Me) were performed with density functional theory (DFT) using the B3LYP hybrid function with the 6-31G* basis set in a Gaussian 09W package on the Shared Hierarchical Academic Research Computer Network (SHARCNET) of Canada. GaussView 5.0 software was used to generate the molecular orbital pictures.

Top-gate, bottom-contact OTFT devices were fabricated on glass wafer (Precision Glass & Optics, Eagle 2000) coated with Polyera ActiveInk™ B2000. The gold source and drain electrodes (~30 nm) were deposited by thermal evaporation using a shadow mask ($L = 50 \mu\text{m}$, $W = 500 \mu\text{m}$). Prior to device fabrication, the substrate was washed with acetone and isopropanol, cleaned by O₂ plasma. The organic semiconductor **3a** or **3b** film was deposited onto the substrates by spin-coating a semiconductor solution in DCB (4 mg mL⁻¹) at 1000 rpm for 30 s and annealed at 110 °C on a hotplate for 5 min in air. Then a 500 nm-thick CYTOP™ dielectric layer (Asahi Glass Co., Ltd.) was spin-coated on top of the semiconductor layer, followed by thermal annealing at 110 °C for 5 min to remove the residual solvent. Subsequently, an 80 nm-thick Ag layer was deposited on the dielectric as a top gate electrode to complete the device fabrication. The OTFT devices were characterized under ambient condition. The carrier mobility in the saturated regime, μ_{sat} , is calculated according to equation (1):

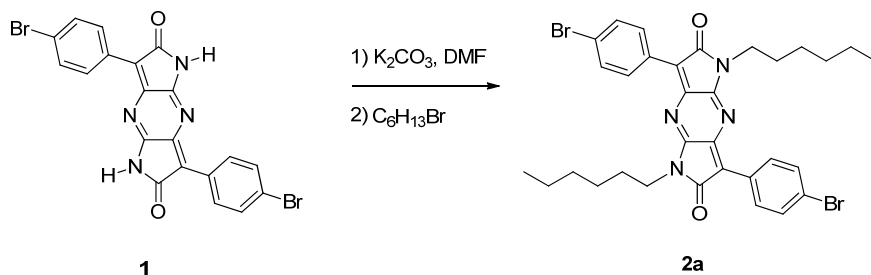
$$I_{\text{DS}} = C_i \mu_{\text{sat}} (W/2L) (V_{\text{G}} - V_{\text{T}})^2 \quad (1)$$

where I_{DS} is the drain current, W and L are the semiconductor channel width and length, respectively, C_i is the capacitance per unit area of the gate dielectric, V_{G} is the gate voltage and V_{T} is the threshold voltage. V_{T} was determined from the V_{G} axis intercept of the linear extrapolation of the $(I_{\text{DS}})^{1/2}$ vs. V_{G} in the saturation regime at $I_{\text{DS}} = 0$.

Supplementary Information

2. Synthetic Procedures

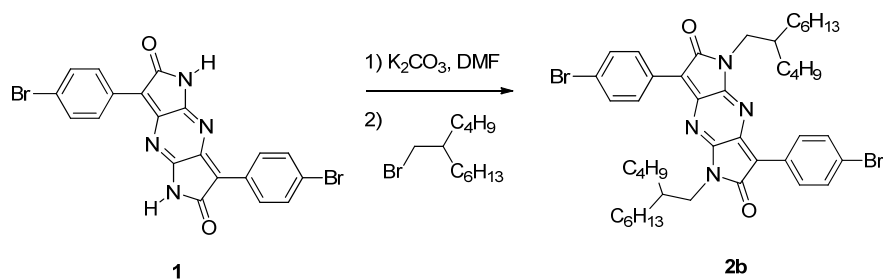
3,7-Bis(4-bromophenyl)-1,5-dihexyldipyrrolo[2,3-*b*:2',3'-*e*]pyrazine-2,6(1*H*,5*H*)-dione (Compound 2a)



In a dry three-necked 25 ml round bottom flask, compound **1** (0.374 g, 0.750 mmol) and anhydrous K_2CO_3 (0.311 g, 2.25 mmol) were suspended in anhydrous *N,N*-dimethylformamide (DMF) (14 ml). 1-Bromohexane (0.385 g, 2.33 mmol) was then added portion-wise and the reaction mixture was further stirred and heated at 130 °C under argon atmosphere. After 8 h, the reaction mixture was allowed to cool down to room temperature, poured into de-ionized (DI) water (120 mL), and stirred for 5 min. The product was extracted with dichloromethane (60 mL \times 3), then washed with water. Removal of the solvent afforded the crude product, which was further purified using silica-gel column chromatography (eluted with CH_2Cl_2). The product was further purified by recrystallization with methanol to give **2a** as a deep red solid. Yield: 0.350 g (70.0 %). 1H -NMR ($CDCl_3$, 300 MHz, ppm): 8.34 (d, 4H, aromatic, $J = 8.7$ Hz), 7.57 (d, 4H, aromatic, $J = 8.7$ Hz), 3.74 (t, 4H, N- CH_2 , $J = 7.2$ Hz), 1.81-1.65 (m, 4H, CH_2), 1.45-1.22 (m, 12H, CH_2), 0.87 (t, 6H, CH_3 , $J = 6.9$ Hz). ^{13}C -NMR ($CDCl_3$, 75 MHz, ppm): 170.25, 160.31, 136.42, 132.03, 131.57, 129.17, 124.85, 120.91, 38.81, 31.44, 28.27, 26.65, 22.65, 14.18.

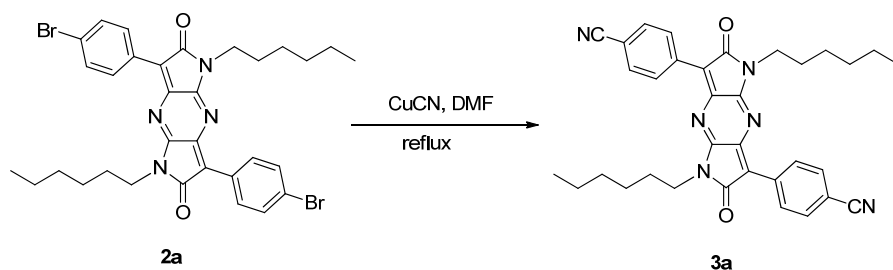
3,7-Bis(4-bromophenyl)-1,5-bis(2-butyl-octyl)dipyrrolo[2,3-*b*:2',3'-*e*]pyrazine-2,6(1*H*,5*H*)-dione (Compound 2b)

Supplementary Information



2b was synthesized from **1** (0.498 g, 1.00 mmol) and 2-butyl-1-octylbromide (0.773 g, 3.10 mmol) using the similar procedure described for **2a**. Yield: 0.438 g (52.5 %). 1H -NMR ($CDCl_3$, 300 MHz, ppm): 8.37 (d, 4H, aromatic, $J = 8.7$ Hz), 7.56 (d, 4H, aromatic, $J = 8.7$ Hz), 3.62 (d, 4H, N- CH_2 , $J = 6.9$ Hz), 2.02-1.87 (m, 2H, CH), 1.50-1.16 (m, 32H, CH_2), 1.00-0.78 (m, 12H, CH_3). ^{13}C -NMR ($CDCl_3$, 75 MHz, ppm): 170.46, 160.49, 136.29, 131.96, 131.57, 129.18, 124.84, 120.69, 42.94, 37.16, 32.03, 31.49, 29.88, 28.11, 26.61, 23.19, 22.83, 14.25.

4,4'-(1,5-Dihexyl-2,6-dioxo-1,2,5,6-tetrahydropyrrolo[2,3-*b*:2',3'-*e*]pyrazine-3,7-diyl)dibenzo nitrile (Compound **3a**)

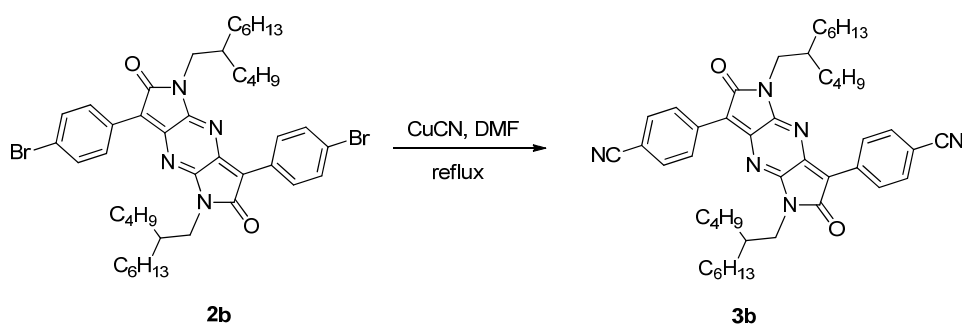


A mixture of **2a** (0.332 g, 0.500 mmol) and cuprous cyanide ($CuCN$) (0.806 g, 9.00 mmol) in 25 mL DMF was stirred under argon at 150 °C for 72 h. The reaction mixture was then cooled down to room temperature, and aqueous ammonium hydroxide solution (300 mL) was added. The brown precipitates were collected by filtration and washed with water. The resulting solid was then dissolved with chloroform and filtered. Evaporation of solvent from the filtrate gave a dark-brown solid, which was further purified using column chromatography on silica (using dichloromethane as the eluent) to afford a brown solid **3a** (113 mg, 40.0 %). 1H -NMR ($CDCl_3$, 300 MHz, ppm): 8.58 (d, 4H, aromatic, $J = 8.7$ Hz),

Supplementary Information

7.73 (d, 4H, aromatic, $J = 8.7$ Hz), 3.79 (t, 4H, N-CH₂, $J = 7.2$ Hz), 1.83-1.69 (m, 4H, CH₂), 1.48-1.20 (m, 12H, CH₂), 0.89 (t, 6H, CH₃, $J = 6.9$ Hz). This compound was not characterized by ¹³C-NMR because of its very poor solubility.

4,4'-(1,5-bis(2-butyloctyl)-2,6-dioxo-1,2,5,6-tetrahydrodipyrrolo[2,3-b:2',3'-e]pyrazine-3,7-diyl)dibenzonitrile (Compound 3b)



3b was synthesized from **2b** (0.250 g, 0.300 mmol) and CuCN (0.484 g, 5.40 mmol) using the similar procedure described for **3a** (71.5 %, 0.156 g). ¹H-NMR (CDCl₃, 300 MHz, ppm): 8.59 (d, 4H, aromatic, $J = 8.7$ Hz), 7.71 (d, 4H, aromatic, $J = 8.7$ Hz), 3.67 (d, 4H, N-CH₂, $J = 6.9$ Hz), 2.04-1.86 (m, 2H, CH), 1.48-1.12 (m, 32H, CH₂), 1.00-0.78 (m, 12H, CH₃). ¹³C-NMR (CDCl₃, 75 MHz, ppm): 170.01, 161.23, 138.06, 134.27, 132.21, 130.42, 119.72, 118.70, 112.95, 43.20, 37.20, 31.99, 31.80, 31.46, 29.83, 28.79, 26.56, 23.16, 22.80, 14.23.

Supplementary Information

3. Additional data:

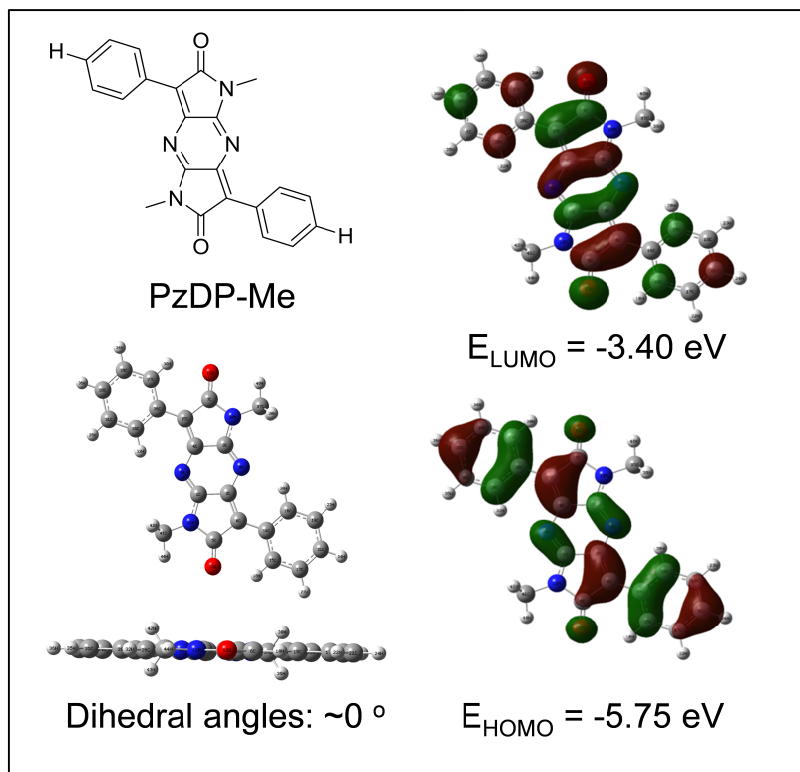


Fig. S1. The optimized structure of PzDP-Me and its LUMO and HOMO energy orbitals obtained by performing density functional theory (DFT) calculations using the B3LYP hybrid function with the 6-31G* basis set.

Supplementary Information

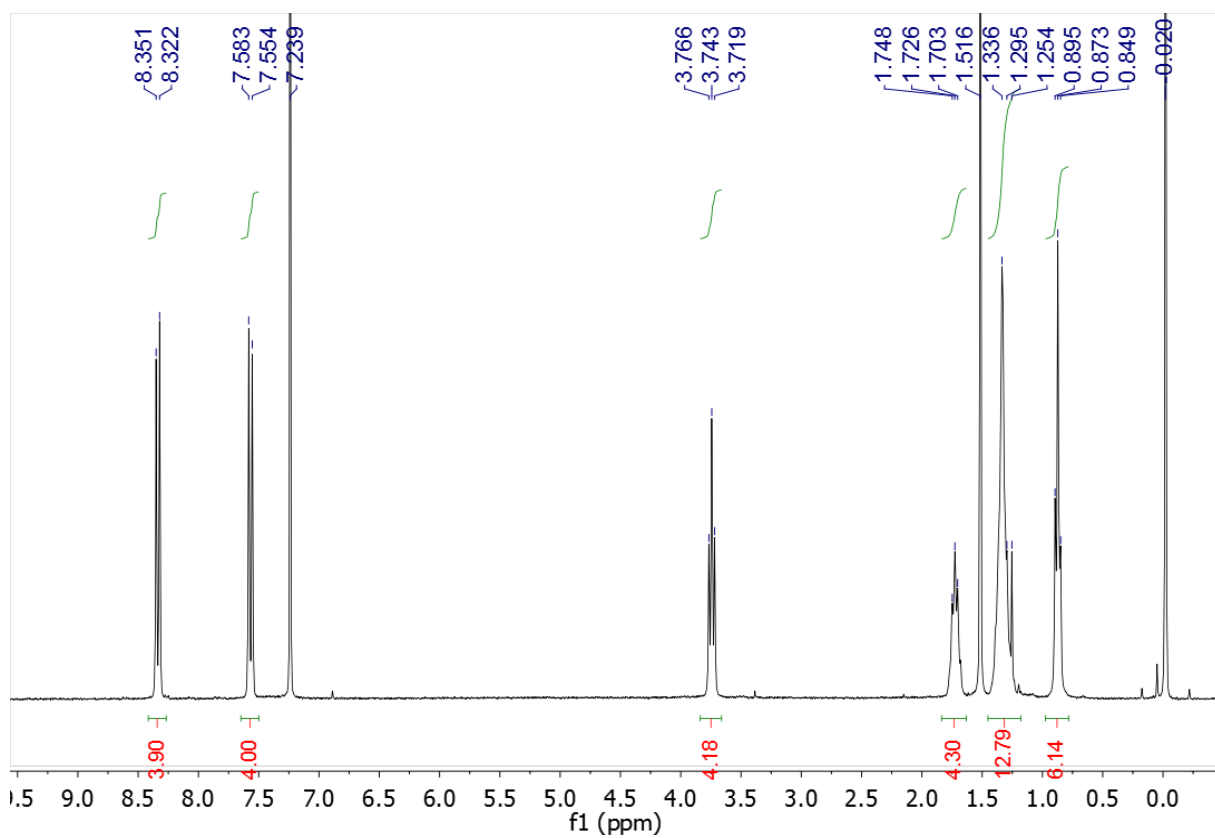
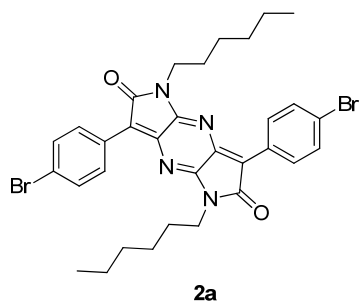


Fig. S2 The 300 MHz ¹H NMR spectrum of compound **2a** measured in CDCl₃.

Supplementary Information

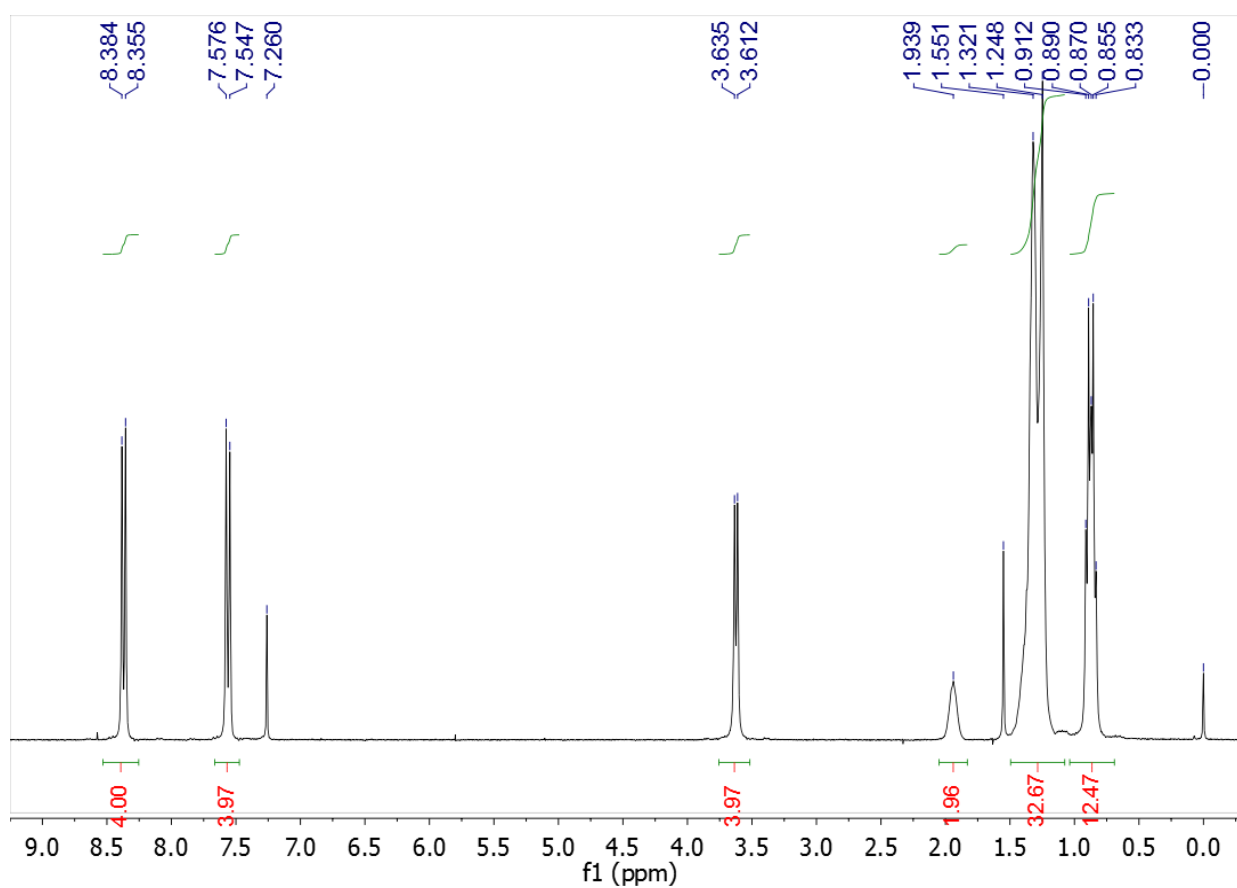
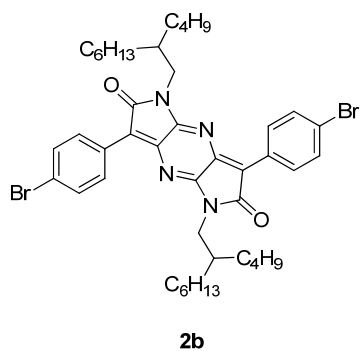


Fig. S3 The 300 MHz ¹H NMR spectrum of compound **2b** measured in CDCl₃.

Supplementary Information

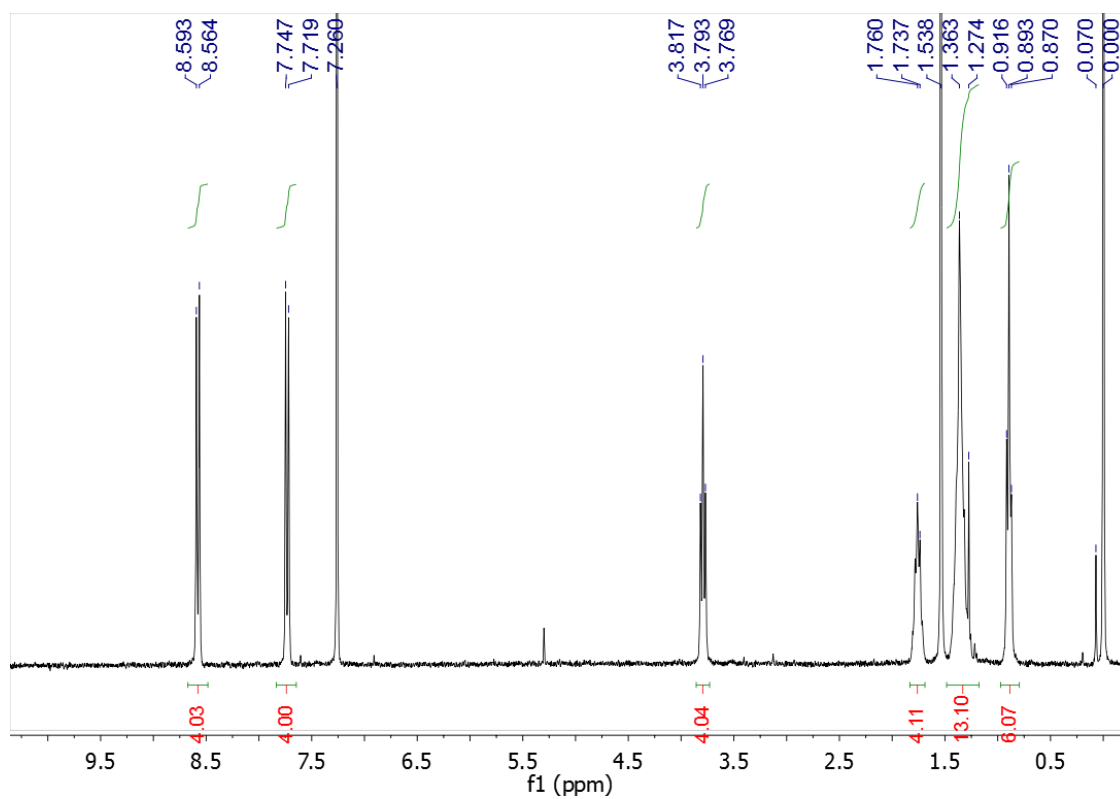
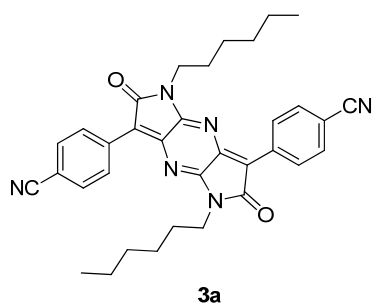


Fig. S4 The 300 MHz ¹H NMR spectrum of compound **3a** measured in CDCl₃.

Supplementary Information

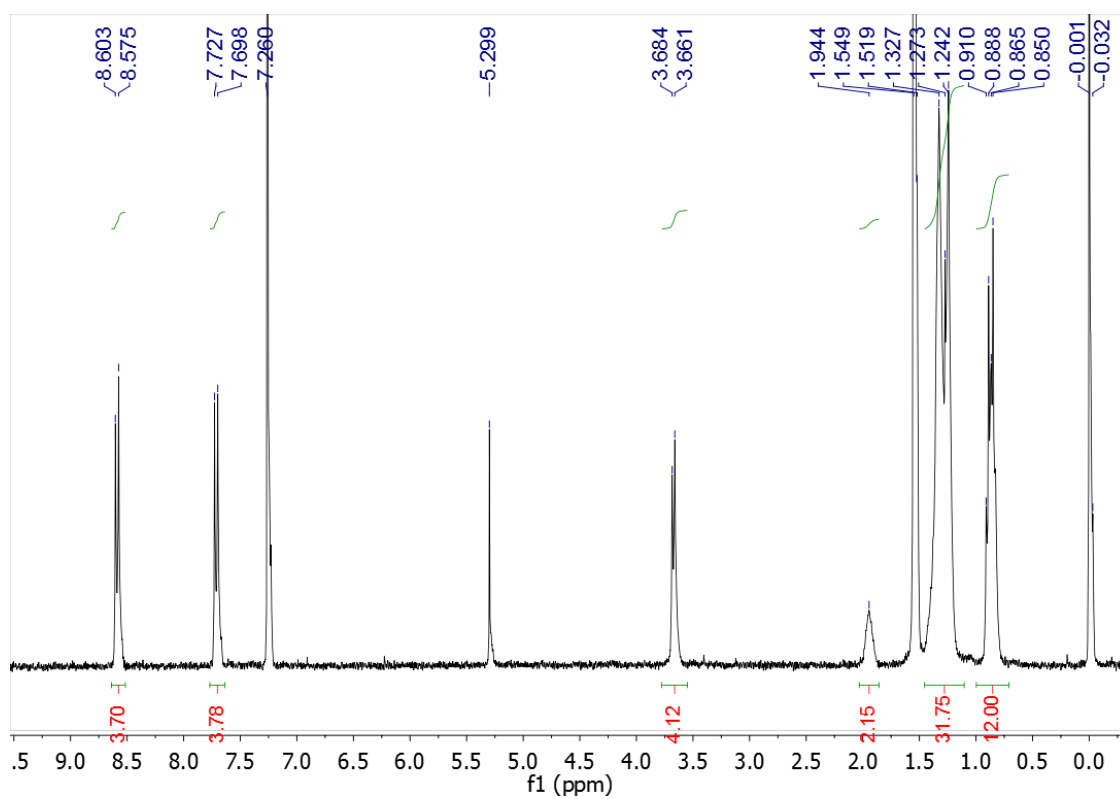
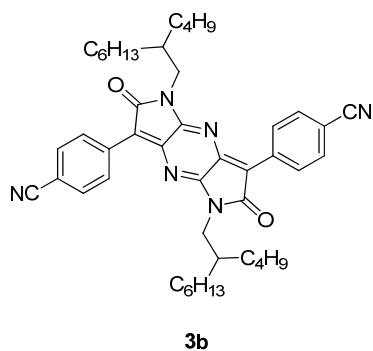


Fig. S5 The 300 MHz ¹H NMR spectrum of compound **3b** measured in CDCl₃.

Supplementary Information

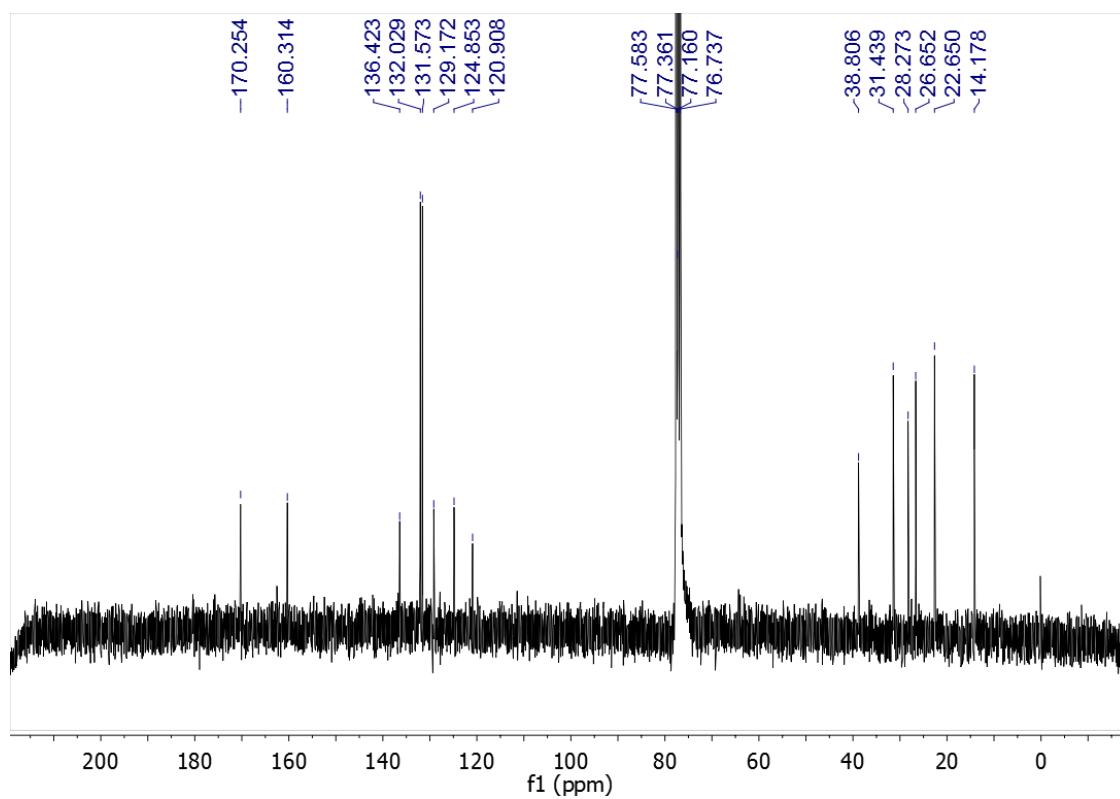
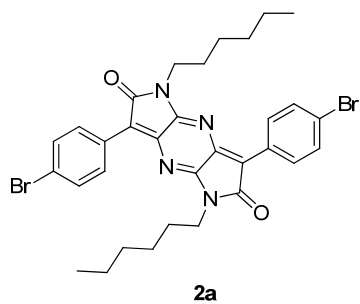


Fig. S6 The 75 MHz ^{13}C NMR spectrum of compound **2a** measured in CDCl_3 .

Supplementary Information

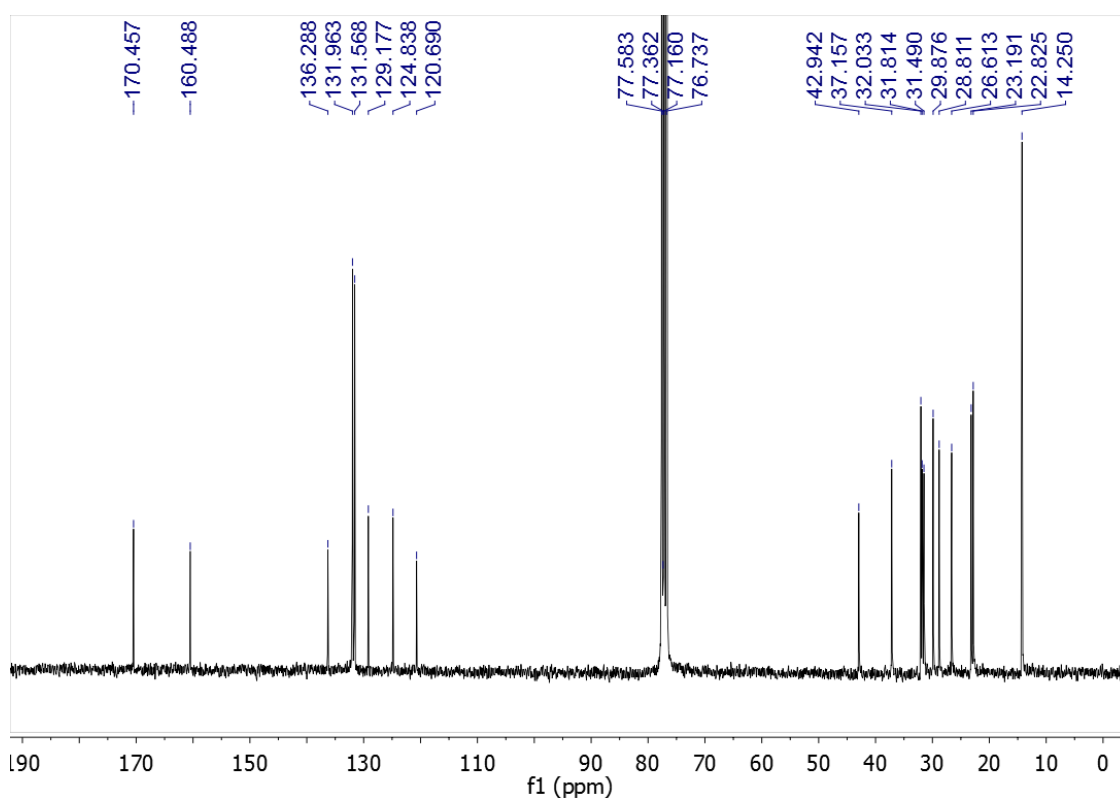
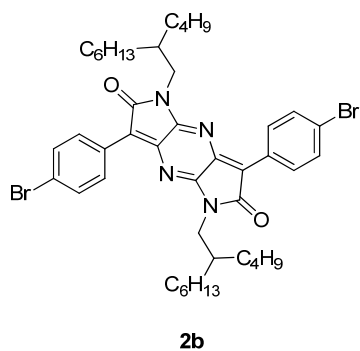


Fig. S7 The 75 MHz ^{13}C NMR spectrum of compound **2b** measured in CDCl_3 .

Supplementary Information

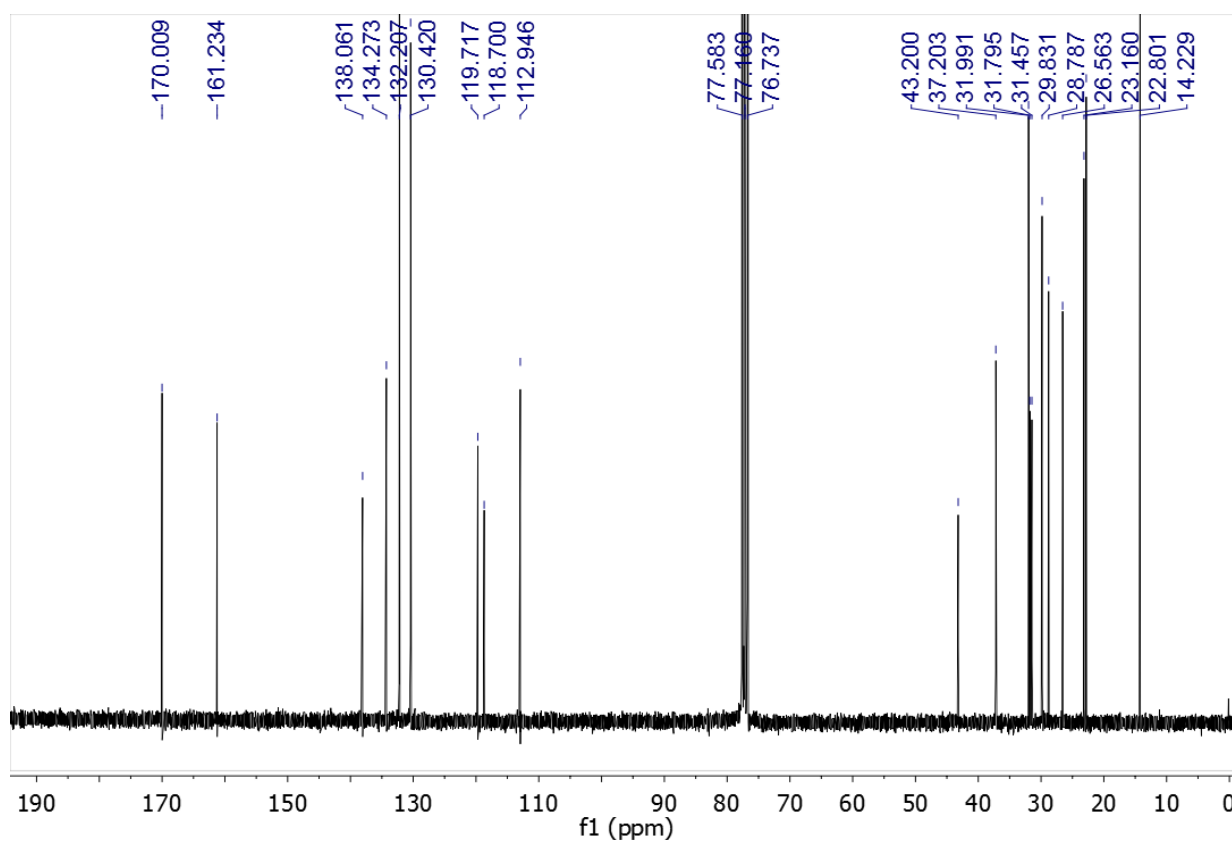
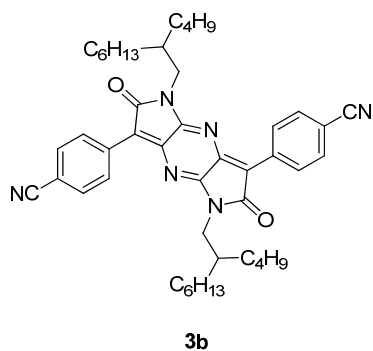


Fig. S8 The 75 MHz ¹³C NMR spectrum of compound **3b** measured in CDCl₃.

Supplementary Information

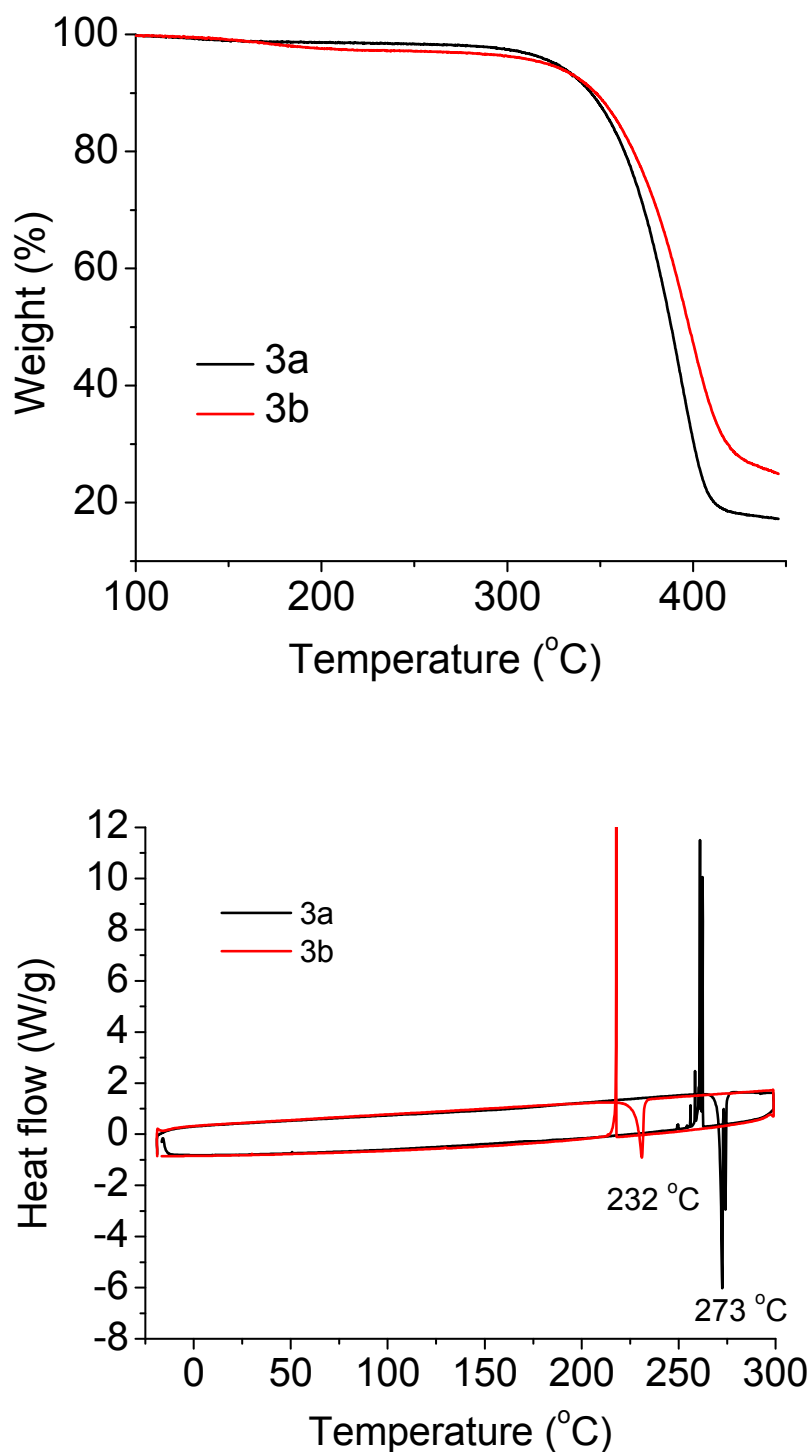


Fig. S9 Thermal analysis data of **3a** and **3b**. Top: TGA curves with a heating rate of $10\text{ }^{\circ}\text{C}\cdot\text{min}^{-1}$ under nitrogen. Bottom: DSC curves with a heating/cooling rate of $10\text{ }^{\circ}\text{C}\cdot\text{min}^{-1}$ under nitrogen.

Supplementary Information

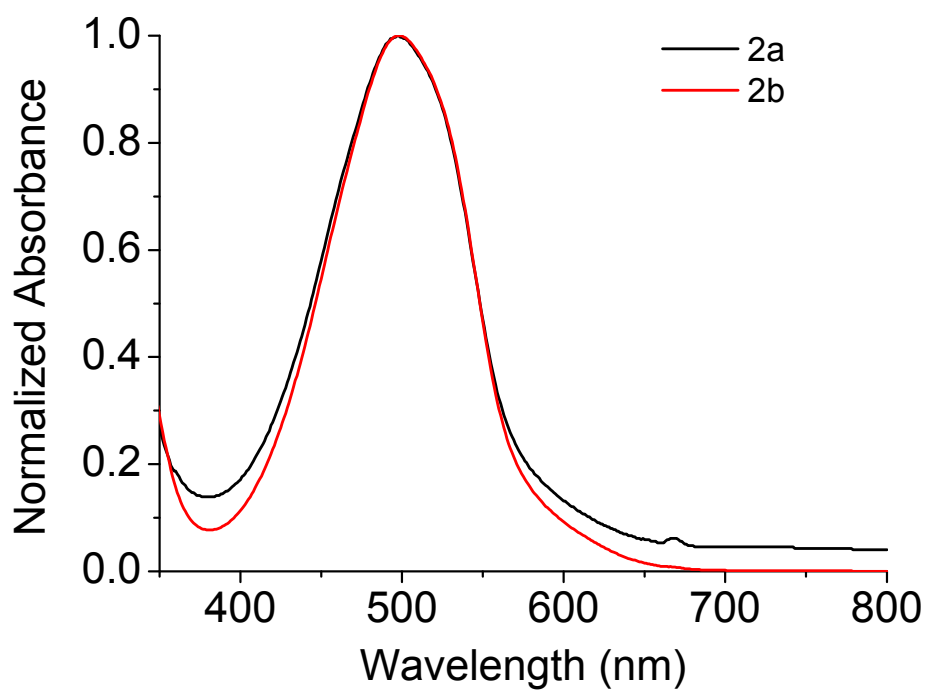


Fig. S10 UV-Vis absorption spectra of **2a** and **2b** in solutions ($\sim 10^{-5}$ M in chloroform).

4. References

-
- ¹ W. Hong, B. Sun, C. Guo, J. Yuen, Y. Li, S. Lu, C. Huang and A. Facchetti, *Chem. Commun.*, 2013, **49**, 484.
 - ² B. W. D'Andrade, S. Datta, S. R. Forrest, P. Djurovich, E. Polikarpov and M. E. Thompson, *Org. Electron.*, 2005, **6**, 11.